Journal of Petroleum Science and Engineering 196 (2021) 108004

Contents lists available at ScienceDirect

Journal of Petroleum Science and Engineering

journal homepage: http://www.elsevier.com/locate/petrol

The fate of hydrocarbon leaks from plugged and abandoned wells by means of natural seepages

Mari R. Tveit [a], Mahmoud Khalifeh [a,*], Tor Nordam [b,c], Arild Saasen [a]

[a] Dept. of Energy and Petroleum Eng., Faculty of Science and Technology, University of Stavanger, Norway
[b] SINTEF Ocean, Trondheim, Norway
[c] Department of Physics, Norwegian University of Science and Technology, Trondheim, Norway

ARTICLE INFO

Keywords:
Fate analysis
Well abandonment
Natural seepages
Zero leak

ABSTRACT

When a well reaches the end of its productive life, it is permanently plugged and abandoned. Even though new technology and verification methods are being evaluated, it is evident that operational, barrier material and qualification challenges together contribute to risk of leaks from abandoned wells or wells to be abandoned in future. Most regulatory authorities constitute zero leak acceptance criteria to protect the environment; however, natural hydrocarbon seepages are occurring all over the world on a daily basis. In this study, we conducted a theoretical comparison between leaking wells and natural seeps and suggest conducting a fate analysis is appropriate to provide necessary data for evaluating environmental implications of leaking wells. Two case studies were analyzed using SINTEF Ocean's OSCAR (Oil Spill Contingency And Response) software; one historical gas leak (Field A) and a theoretical oil leak (Field B). It is found that for releases of natural gas, 95–99% dissolve in the ocean, and the fraction of gas reaching the atmosphere is dependent on the initial gas bubble size. Fate of oil is more complex than gas, but evaporation, sedimentation and biodegradation are the main contributing mechanisms in the fate of hydrocarbon analysis.

1. Introduction

When a well reaches the end of its lifecycle, and it is not to be re-used or re-entered, it becomes subject to Permanent Plug & Abandonment (PP&A). Different regulatory authorities around the world have different requirements to be fulfilled when plugging and abandoning a well, and operators must comply with the local standards (IEA GHG, 2009). Even though no global standards exist, the common intention of PP&A is to maintain well integrity in an eternal perspective, as stated by Norwegian well integrity standard NORSOK D-010 (2013). Additionally, all freshwater zones and hydrocarbon bearing zones in the overburden must be isolated and protected, and finally the pipes must be cut and retrieved to an agreed level below seabed or ground, in order to leave the well in a condition such that both the downhole and surface conditions are protected (Campbell and Smith, 2013). Generally, most regulatory authorities require two independent, permanent well barriers to be placed over hydrocarbon-bearing or abnormally pressured zones and one permanent well barrier for non-hydrocarbon potentials. The well barriers must be extended from formation to formation, prevent flow in both vertical and lateral direction and maintain a permanent seal (NORSOK D-010, 2013; Oil & Gas UK, 2012a). Ordinary Portland Cement (OPC) is currently and historically the prime material used for creating permanent well barriers, however, other materials can also be used if they fulfill the main requirements of a barrier material (Oil & Gas UK, 2012b; Khalifeh et al., 2013; NORSOK D-010, 2013):

- Impermeable – prevent unwanted flow of hydrocarbons or over-pressured fluids through the barrier.
- Long-term integrity – does not deteriorate over time
- Non-shrinking – no unwanted flow between plug and casing or annulus.
- Ductile – able to withstand mechanical loads and changes in temperature and pressure.
- Resistance to downhole fluids and gases (corrosive gases as CO_2, H_2S, hydrocarbons etc.).
- Able to make a good bond to the formation or casing in which the barrier material is placed.

The most highly regulated areas for well abandonment are the North Sea and the Gulf of Mexico (GoM). Both are areas with long oil and gas production history, ageing infrastructure and fields near reaching the

* Corresponding author.
E-mail address: Mahmoud.khalifeh@uis.no (M. Khalifeh).

https://doi.org/10.1016/j.petrol.2020.108004
Received 1 July 2020; Received in revised form 27 September 2020; Accepted 28 September 2020
Available online 2 October 2020

Nomenclature

COP	Coal Oil Point
GoM	Gulf of Mexico
MEMW	Marine Environmental Modeling Workbench
NCS	Norwegian Continental Shelf
OPC	Ordinary Portland Cement
OSCAR	Oil Spill Contingency And Response
PP&A	Permanent Plug and Abandonment

end of their productive lives (Smith et al., 2011). The North Sea is divided into sectors between the surrounding countries, with the dominating petroleum producing sectors being the United Kingdom, Norwegian, Dutch and Danish sectors. Each country has its own regulatory authorities, and they are The Health and Safety Executive, the Norwegian Petroleum Directorate (NPD), the Dutch Supervision of Mines and the Danish Energy Agency (DEA), respectively (Fronks, 2002; IEA GHG, 2009). They all require zero leak criteria for permanently abandoned wells. However, even though their objectives are the same and they are supervising sectors within the same geographical area, the authorities have different requirements to well barriers in permanent plug and abandonment operations, particularly regarding the length of the barriers. While the Norwegian and Dutch well integrity standards both require 100 m of cement in open hole and 50 m of cement above a mechanical plug, the UK guidelines generally require 500 ft of cement with a minimum window of good quality cement of 100 ft (30.48 m) (Liversidge et al., 2006; NORSOK, 2013; Oil & Gas UK, 2012a).

OPC is well suited for use in wells, as the hydration process can take place submerged in water and the development of strength is predictable, uniform and relatively rapid. Set cement has low permeability and is near insoluble in water. By using different additives, systems for well cementing can be designed for a wide range of temperatures and pressures. OPC is also an inexpensive material, and it is therefore used in almost all well cementing operations (Nelson and Guillot). However, OPC does not actually fulfill all the requirements of a barrier material. It cannot withstand high temperatures and corrosive environments, which may lead to gas influx unless certain chemicals or additives is added (Vignes, 2011). Cement is also known for becoming brittle after setting, and can experience bulk shrinkage during setting, typically in the range of 0.5–5.0% (Salehi et al., 2016; Nelson and Guillot, 2006). These challenges can be mitigated by adding different additives, and optimizing the cement slurry for each individual operation (Lende, 2012).

There are numerous parameters during cementing operations that may influence the long-term sealing capacity, and consequently affect well integrity. In addition to designing the cement slurry, operational parameters must be optimized to achieve satisfactory results (Barclay, 2001). Failure to do so may lead to barrier failure. There are three possible barrier failure modes: leakage around the bulk material, leakage through the bulk material and shift in barrier position. A schematic of potential leak paths is shown in Fig. 1.

There are several possible mechanisms that may cause leakage paths to form, both during and after the plugging operation. During setting, loss of fluid from the cement slurry to the formation may cause gas intrusion to the cement slurry, allowing gas channels to form. Bulk shrinkage during setting may also create small cracks and gaps or microannuli that may become leak paths for leaking hydrocarbons (Barclay et al., 2001). The hydraulic bonding strength, the ability to prevent flow between the cement and the casing or formation, may be drastically reduced by inadequate hole cleaning pre-cementing (Khalifeh et al., 2018; Evans and Carter, 1962). Even when successful in creating a strong hydraulic bond, this may fail in time in a process called debonding. Debonding can occur as a result of various processes and factors, many of which are outside the operator's control, such as

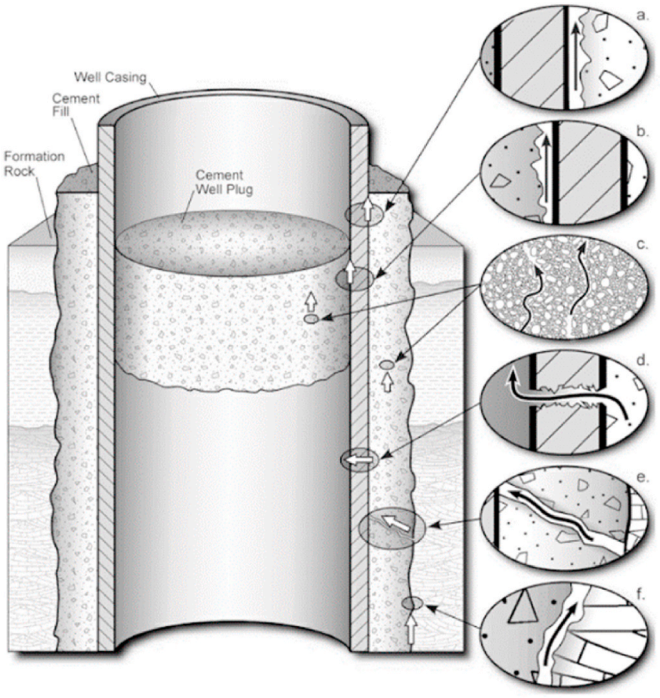

Fig. 1. Possible leakage pathways through an abandoned well. Figure reproduced from Gasda et al. (2004).

changes in the tectonic stresses in the formation, subsidence, pressure decrease during production, pressure build-up post-PP&A, stimulation practices and temperature fluctuations or cement shrinkage with time (Thiercelin et al., 1998; Nelson and Guillot, 2006).

After cementing, the quality of the barrier should be tested in accordance with the well integrity standards. Today's barrier testing and verification methods, such as tagging, pressure testing and use of cement bond logs (CBL) and variable density logs (VDL), all provide qualitative measurements (Khalifeh et al., 2017). They are not capable of giving quantitative measurements on cement quality, and combined with the aforementioned material and operational challenges, it is evident that a risk of leaks is present. Even though NORSOK D-010 (2013) provides zero leak acceptance criteria for abandoned wells, there are no requirements of monitoring systems for abandoned wells, and how to proceed in the case of a leak is unclear. As the wellhead is removed in the last stage of PP&A, re-entering an abandoned well in a safe matter to do a re-abandonment would be time consuming, difficult and extremely costly. Today's regulations do not address this topic, and the current work is therefore meant to serve as a source of information to help the industry form new, more specific standards and evaluation processes in the case of leaking wells. Two case studies have been performed, investigating one historical gas leak case and one theoretical oil leak case. To be able to evaluate the consequences of leaking wells, the cases are placed in the context of natural hydrocarbon seepages; a well-known, natural phenomenon.

1.1. Natural hydrocarbon seepages

On every continent, hydrocarbons are naturally and spontaneously emerging at the surface (Etiope, 2015; Judd and Hovland, 2007). These natural oil and gas seeps occur both onshore and offshore as indications of over-filling of some conventional reservoirs or geological interruptions such as faults, natural fractures or other natural events, and a map compiled of reported seeps is shown in Fig. 2.

Natural seeps are the oldest oil and gas prospecting tools, and in the beginning of the oil industry, all exploration activities were focused around wells being dug or drilled near seeps. In Burma, oil production

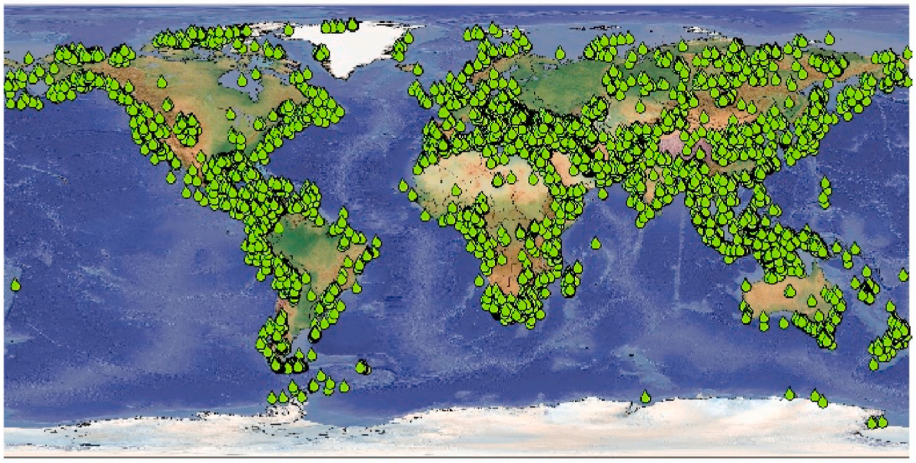

Fig. 2. Map of reported oil and gas seeps created from global data sets. Reproduced from CGG Geoconsulting (2015).

started as early as 1800 from 500 hand-dug wells in what is now called the Yenangyaong field. The name of the field is said to mean "town through which flows a river of oil". In Iran, every field was associated with surface oil and gas seeps up until 1949 (Link, 1952). Even though technology has progressed and there now exist more sophisticated ways of exploration, studying hydrocarbon seepage is still used for identifying commercial sources of petroleum (Logan et al., 2010).

The terms *seep* and *seepage* are often used interchangeably, although their definitions are different. The term seep indicates fluid emerging from a point source, with a flowrate that can be expressed as mass per time, for instance grams day^{-1}. The term seepage on the other hand, is used to denote the phenomenon or geological activity and to provide information on the flowrate from an aerial source, with a flowrate that can be expressed as mass per time per area, for instance gram m^{-2} day^{-1} (Etiope, 2015). Seepage can appear as either *macro-seeps* or *micro-seeps*, where macro-seeps produce focused streams of gas bubbles or oil droplets. This focused migration is generally an indication of a subsurface with fractures or faults that make up migration routes. Offshore macro-seeps can therefore be both visually and acoustically detected (Hovland et al., 2012). Micro-seep is evidence of a more widespread, dispersed exhalation of gas through a permeable subsurface, usually detected by taking samples of sediment pore water or measuring dissolved gas concentrations in the seawater above the expected seepage area (Etiope, 2015). For the current work, offshore macro-seeps are studied as they are the ones most similar to the case of leaking wells.

Conventional oil and gas are products of catagenesis, the thermal cracking of organic matter into smaller hydrocarbons. This process usually occurs when organic matter is preserved and subject to deep burial and temperatures above 60 °C, and the resulting oil and gas is named thermogenic hydrocarbon. Natural gas can also be produced by microbial communities in shallow sediments, a process called diagenesis. This process can occur in relatively low temperatures, typically 60–80 °C, and the resulting shallow gas is commonly known as biogenic or microbial gas (Tissot and Welte, 1984).

When studying seeping gas, it is desirable to know the origin of the gas. The gas can be classified by examining the stable isotopes of carbon ($^{13}C/^{12}C$) and hydrogen ($^{2}H/^{1}H$) in methane, commonly expressed as $\delta^{13}C$ and $\delta^{2}H$ in % relative to the Vienna Pee Dee Belemnite (VPDB) and Vienna Standard Mean Ocean Water (SMOW) standards (Schoell, 1980). The distributions of carbon and hydrogen isotopes are well defined for thermogenic and biogenic gas worldwide; biogenic gas is generally characterized by $\delta^{13}C$ values below −50%, while $\delta^{13}C$ values for thermogenic gas are generally in the range of −45 to −30%. $\delta^{13}C$ and $\delta^{2}H$ values of a gas are usually plotted together in a Schoell's diagram, where different fields denote biogenic, thermogenic and mixed source gas (Stolper et al., 2018). The Bernard ratio, $C_1/(C_2+C_3)$, is also often used in classifying seeping gas, and describes the compositional differences between biogenic and thermogenic gas by denoting the relative abundance of light hydrocarbons (Bernard et al., 1978). Typically biogenic gas will consist mostly of methane and has a Bernard ratio >500, while thermogenic gas often includes heavier hydrocarbons up to hexane (C_6) and has Bernard ratio <100. Note that these values vary slightly in the literature, ranging from biogenic gas >1000 and thermogenic gas <50 (Brooks et al., 1979; Etiope, 2015). Highly mature and dry thermogenic gas may in some cases have Bernard ratio high enough to be mistaken for biogenic gas. To avoid misinterpreting the ratio, it is therefore common to plot the isotopic signature $\delta^{13}C$ towards the Bernard ratio in a Bernard diagram. This diagram can also be useful to determine if seeping gas may be a mixture originating of deep, thermogenic sources and shallow, biogenic sources.

There are several spots along the coast of Norway where natural gas seepage has been detected. Chand et al. (2008) have found an active seepage system from a believed reservoir on the continental shelf outside Vesterålen, there is gas actively venting from hydrate systems on the Vestnesa ridge off the western coast of Svalbard and gas leakage is also present in the Barents sea at the Snøhvit field (Bunz et al., 2012; Mohammedyasin et al., 2016). Within the central and northern North Sea, there are three well-known macro-seeps that have been subject to numerous studies, including the Gullfaks and Tommeliten seep areas in the Norwegian sector and the Scanner pockmark seeps in the UK sector (Hovland et al., 2012).

Even though there is a large amount of recorded seepage on the NCS, there are few detailed studies including flux rate measurements, and this pattern is recognizable all over the world. To measure the flux from a seep or seep area, considerable amounts of time and money are needed to install necessary equipment over each individual vent or bubble flux. Furthermore, a representative number of vents must be evaluated within a time frame large enough to include all spatial and temporal variations (Judd, 2004). Common flux measurement equipment includes cameras, rulers and funnels; by filming a vent and observing the sizes and the frequency of the bubbles released, it becomes possible to calculate the volume of gas released (Schneider von Deimling et al., 2011). Such studies have been conducted at the Scanner pockmarks and the Tommeliten seep area. For the current work, emphasis is placed on the studies from the Tommeliten seep area, due to the low activity and flux rates measured at the Scanner pockmarks.

The seeps at Tommeliten were first discovered in 1978 after a routine site survey. Side scan sonar records indicated that gas emanated as bubbles from the seafloor in an area over a salt diapir structure. The salt structure was near circular, 3 km wide and located approximately 1000

m below the seafloor. On shallow seismic records, plumes of bubbles were visible in the water column, and acoustic scattering and chaotic reflections above the salt diapir constituted evidence of gas charged sediments, sparking the interest for doing seabed surveys (Hovland and Sommerville, 1985). In 1983, a detailed survey with a Remotely Operated Vehicle (ROV) was performed, measuring 10 mm diameter bubbles emerging every 6th second from an estimated 120 vents. The total flux corresponded to 51 t/yr. Measured $\delta^{13}C$ values of −45.6% and presence of heavier gas molecules up to pentane (C_5) suggested a thermogenic origin of the gas (Hovland and Sommerville, 1985; Hovland et al., 2012). A new, detailed survey to reassess the mass flux was published in 2011, this estimates the total seepage rate for the Tommeliten area to be 26.3 t/yr, approximately half of the previous study. With a density of 0.671 kg/m^3, this equals 4474.3 L/h. At this point, the average diameter of the seeping gas bubbles was measured at 4.5 mm, and the gas ebullition was of uniform character and size (Schneider von Deimling et al., 2011).

There are currently no available data documenting oil seeps off the Norwegian coast, which according to Judd and Hovland (2007) might be a result of the geology of the subsurface, that has few obvious leakage paths. This is a contrast to the most prolific offshore oil seep areas in the world, namely the GoM and offshore California. In the GoM, prolific seepage is made possible by the presence of near-surface faulting associated with the extensive amount of salt domes and diapirs, which also make up some of the largest reservoirs in the area. Renewed or persisting salt movements are a continuous source of leakage paths for seeping oil and gas (Geyer and Sweet, 1972). The heavy seepage affects several aspects of the local environment. On the seafloor, tar mounds and asphalt mud volcanoes are widely reported, while floating tar balls drift to shore and contaminate local beaches. In seep areas, seabed piston cores have yielded up to 15% oil by weight and hold gases with thermogenic isotope signatures, and tar has been found in sediments in more than 3000 m water depth (US National Research Council, 2003). The total GoM oil seepage rates have been attempted quantified several times by mapping oil slicks on surface using satellite remote sensing. In the 1990s, estimates ranged between 4000 and 17,000 ton per year. In 2003, Kvenvolden and Cooper (2003) found that a likely estimation for the total GoM seepage rate is about 140,000 ton per year. The estimate was based on the assumption that the average thickness of the oil slicks are 0.1 μm, and that oil persists on the surface for 12 h before evaporation. Even though temporal variations and weather patterns were not taken into account, it is evident that the GoM is a prolific seepage area.

Large oil slicks are also common offshore California, extending up to 10 km in length (Mikolaj et al., 1972). The most intense area of seepage is known as the Coal Oil Point (COP), a point overlying anticlinal structures containing oil in the Monterey formation. The cap rock above it, the Sisquoc formation, is heavily fractured, allowing oil to seep up to from the reservoirs. Hornafius et al. (1999) made an estimation of the total oil seepage from COP by combining data from seep tents, seep flux buoys floating in the seep area and 50 kHz sonar data, and stated that annual seepage was in the range of 7800 to 8900 ton. With estimates for total oil seepage offshore California at 17,000 ton per year, COP is responsible for roughly 50% of the total seepage in the area (Kvenvolden and Cooper, 2003). Oil and gas often seep from the same vents, and in COP seepage primarily appears as oil-coated gas bubbles (Leifer and Boles, 2005). The resulting low density effectively transports oil to the surface by buoyancy, where surface oil slicks are known to negatively affect marine life such as seals and seabirds and be a source of contamination to beaches and local shorelines (Mikolaj et al., 1972; SOS California, 2018).

1.2. Fate modeling

Fate modeling is the first step when trying to understand how leaking oil and gas from abandoned wells may affect the surroundings, and gives a quantitative analysis of how the hydrocarbons behave and fractionate in the environment. Gas released as bubbles from the seafloor will rise vertically due to buoyancy, and upon rising, be subject to dissolution. The mass transfer between gas bubbles and seawater is a function of several variables, including, but are not limited to, bubble size, diffusivity, level of contamination in the liquid, water depth, salinity, ambient temperature and pressure (Olsen et al., 2017).

The fate of oil releases is more complex. Released oil will undergo a series of chemical and physical changes, commonly called weathering processes. Weathering includes the processes of evaporation, dispersion, dissolution, emulsification, oxidation, sedimentation and biodegradation, as visualized in Fig. 3 (Lindo-Atichati et al., 2016; WHOI, 2014).

When oil emerges from the seafloor, either as a leak or a natural seep, it will rise upwards through the water due to buoyancy effects, as oil is usually lighter than the surrounding water. Upon reaching the surface, the oil spreads and forms surface slicks, from where the lighter components may evaporate. The fate and extent of an oil slick are dependent on wind and wave activity, as breaking waves may force oil downwards in the water column (Nissanka and Yapa, 2017). Thus, the fraction of oil on the surface is larger in calmer weather, and typically larger in summer than in winter. The evaporation rate of the oil is mainly dependent on the chemical composition, as lighter compounds are more willing to enter gaseous phase than heavier compounds. This willingness is however affected by the ambient temperature, increasing evaporation rates in summer (Fingas, 2011).

As the lighter components evaporate, the remaining surface oil is enriched in heavier components until the point where the bulk density is likely to exceed water density. Consequently, the heavier oil compounds sink and may ultimately settle and be deposited on the seafloor sediments (Farwell et al., 2009). The sediment deposition often occurs some distance from the origin of the release, as the oil slick is transported with wind and currents for some time before the evaporation and subsequent enrichment and sinking of the heavier compounds take place, as shown in Fig. 3.

Both while rising and sinking, oil submerged in water is subject to dispersion and dissolution processes. Natural dispersion occurs when wave action or turbulence causes the oil to break up into fine droplets and transfers them into the surrounding water. Oil droplets with a diameter smaller than 20 μm are typically relatively stable in water, and will remain so for large periods of time, and are thus able to be transported over large distances by the currents (US National Research Council, 2003). Heavy oils are not likely to disperse naturally, whereas lighter oils or refined oil products may disperse almost completely if the asphaltene and resin contents are low. As dispersion is an effect of significant wave action and energetic seas, dispersion is more likely to occur during winter than in summer.

The dissolution process is the chemical stabilization of oil components in water. It is considered to be an important process, as the most soluble compounds of oil, light aromatic compounds, are also commonly the most toxic compounds. Solubility decreases rapidly with increasing molecule size, and the dissolution rate may also be affected by the sizes of the oil droplets. When dissolved, oil becomes more prone to oxidation effects, the process of altering the chemical composition of the oil by either light-catalyzed reactions (photooxidation) or microorganisms in the seawater (microbial oxidation). Given unrestricted time and oxygen supply, the ultimate fate of oxidation is the conversion of oil compounds into carbon dioxide and water:

$$CH_2O + O_2 \rightarrow CO_2 + H_2O$$

where CH_2O is a symbol for all organic compounds. Photooxidation occurs when sunlight acts on oil in the surface layers, but the mechanism is not well understood, nor considered an important part of the weathering processes (Fingas, 2011). Microbial oxidation is of much greater importance and is perhaps more commonly referred to as biodegradation. Various species of yeast, fungi and bacteria are capable of metabolizing different hydrocarbons as a food energy source. These organisms

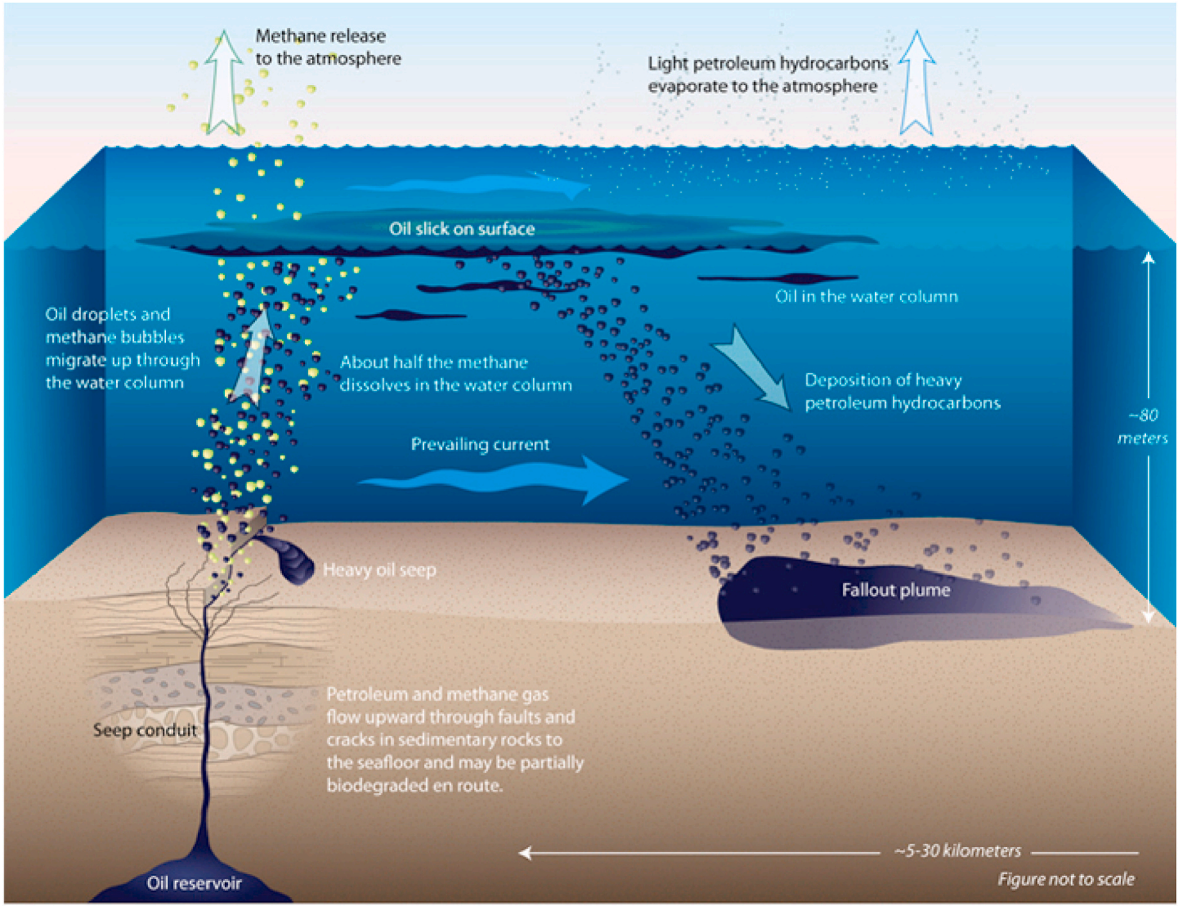

Fig. 3. Fate of naturally seeping oil and gas. Reproduced from © Woods Hole Oceanographic Institution, J. Cook (2014).

are present everywhere in the environment, but most prolific in seep areas. The rate of biodegradation primarily depends on the nature of the hydrocarbons; saturated alkanes, particularly those with carbon number 12 to 20, or smaller aromatics are often consumed first, while branched alkanes, multi-ring aromatics and polar compounds containing sulfur or nitrogen are more resistant to biodegradation (US National Research Council, 2003). Oxygen supply and ambient temperature also affect the biodegradation rate, and in general, biodegradation rates tend to increase with increasing temperature (Nordam et al., 2020; Bagi et al., 2013). However, for some oils biodegradation can be a very slow process, allowing oil to persist in the environment for years. Therefore, biodegradation is not considered an important weathering process in the short term (Fingas, 2011).

To summarize, the fate of leaking oil and gas is dependent on numerous factors, including chemical composition of the fluid, characteristics of the release, the environmental parameters including weather and seasonal variations and the variety of marine organisms present in the area.

2. Methodology

2.1. Software

The software used for this study is Oil Spill Contingency And Response (OSCAR) and the associated gas-tracking module Gastrack, both part of the Marine Environmental Modeling Workbench (MEMW) provided by Norwegian research institute SINTEF Ocean. MEMW is a framework of software used for analyzing releases of various pollutants to the marine environment, including chemicals, hydrocarbon leaks, blowouts and contamination from drill cuttings. The software is a result of many years of research following the Ekofisk blowout in April 1977. In seven days, 13,000 t of oil was released to the sea. Luckily the release caused less damage than feared; as the released oil was light, it evaporated and dispersed naturally before reaching shore (Audunson, 1980). However, it sparked an interest for oil spill research and development on the NCS, and since 1978, approximately 40 experimental oil spills have been conducted in Norwegian waters, including both large and small releases in open and ice covered waters. By releasing and tracking oil by ship or air craft, valuable information about how it spreads, disperses and fractionates can be obtained, and together with theoretical modeling, laboratory testing and basin studies, this forms a strong foundation for the MEMW models (Faksness et al., 2016).

The OSCAR model was made for quantifying environmental consequences of oil spills and the effectiveness of various response strategies and computes the fate and weathering of oil after release. The user sets up a release scenario, where depth, rate and duration of the release are entered, together with exact coordinates and a chosen grid and computational time step for the simulation. The MEMW models use particles to compute behavior, transport and effects of pollutants, and particles can be strictly Lagrangian or “pseudo-Lagrangian”, where the first represent passively transported particles subject to the advection and turbulence of the surrounding water, such as dissolved substances or drifting plankton, and the latter typically represents droplets in water, which are additionally subject to vertical rising or settling velocity (SINTEF, 2017).

Environmental parameters are important input for the simulations. For analyzing the oil and gas leaks presented in this work, a location database of Northern Europe have been provided, together with an ocean depth database including bathymetry data and a database containing properties of more than 130 oils and petroleum products,

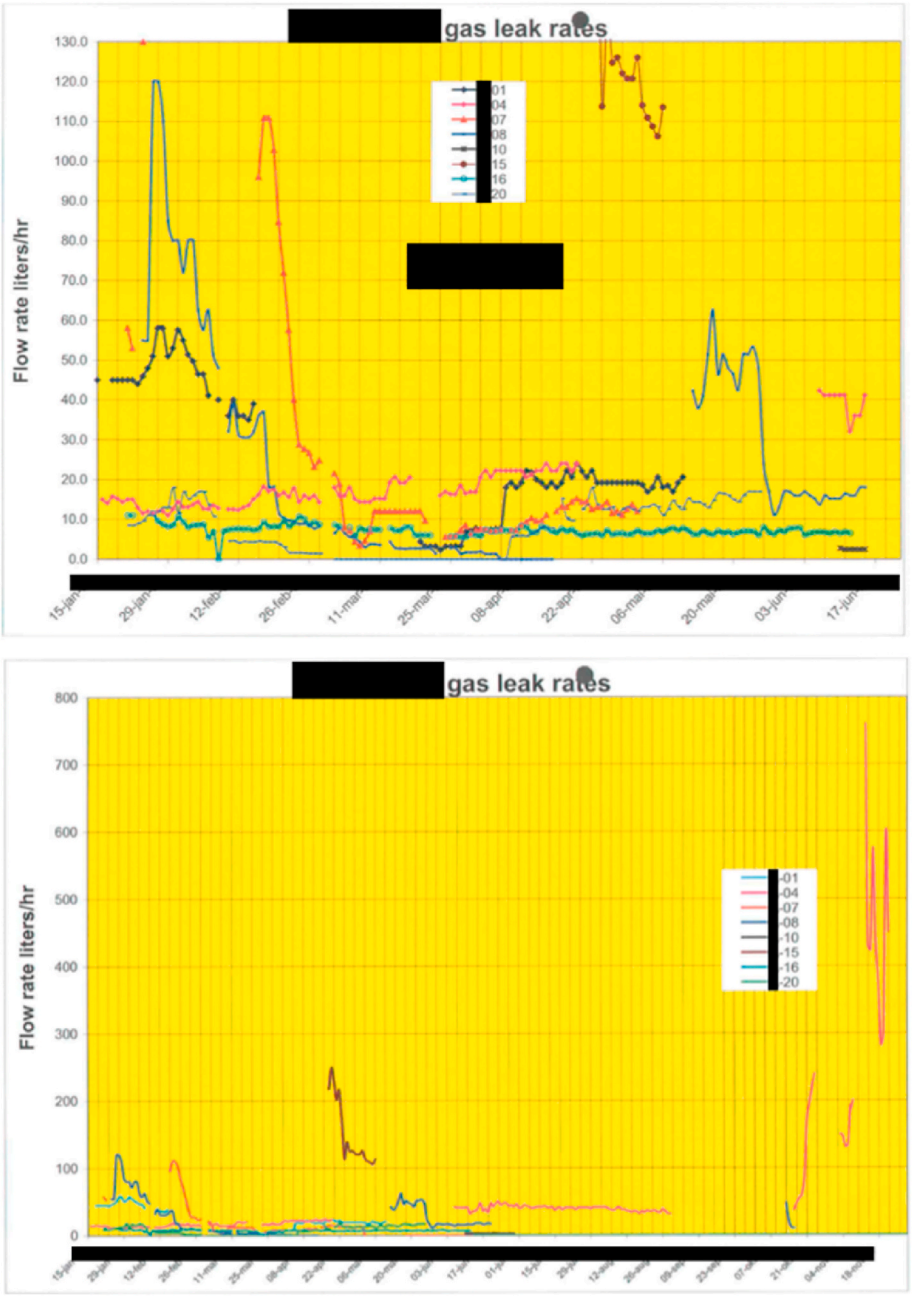

Fig. 4. Monitored leak rates for the different wells prior to re-abandonment.

including all Norwegian North Sea oils. Properties include chemical composition, viscosity and API gravity (SINTEF, 2017). Current and wind data were also provided as a courtesy of SINTEF and were produced using the SINMOD hydrodynamic model (Slagstad and McClimans, 2005). Datasets describing atmospheric temperature and temperature and salinity profiles for the water column were downloaded from The Norwegian Meteorological Institute's open access databases[1]. To account for seasonal variations in the fate analysis, both winter and summer simulations have been performed for all leakage scenarios. There are strong seasonal variations in the hydrographic conditions in the entire central and northern offshore areas of the North Sea. As spring and summer progress, warming of the atmosphere and reduced storm activities cause the reduction of vertical mixing in the water column and the heating of the upper water layers. A thermocline forms, a thin zone dividing the warmer, upper mixed layers and the calmer, colder water below, gradually suppressing vertical exchange between the deep and shallow water (Schneider von Deimling et al., 2011). After cooling starts in October, paired with increasing wind speed, the water column is destabilized, and the thermocline will fade and disappear. In February, the water column will be near homogenous and vertical mixing will be at maximum level (Pohlmann, 1996).

2.2. Case study A

Case study A is a historical gas leak case from the NCS. Data have been provided by an undisclosed, Norwegian operator that some years ago chose to permanently plug and abandon all wells from a platform after roughly 20 years of gas production. The platform was located in approximately 70 m water depth at what is henceforth called Field A.

[1] https://thredds.met.no/.

During abandonment, cement plugs were placed inside the casings and the existing annular cement was used as part of the well barrier. After the PP&A campaign, leaks in all wells were experienced. As the leaking gas was of thermogenic origin and migrating through the original casing cement between the 13 3/8" and 20" casing, it was believed that the annular cement had been gas cut during primary cementing, allowing channels to form in the cement. To correct the leaks, the operator decided that all wells needed section milling and placing of new open hole formation to formation plugs, consequently more than doubling the cost of the PP&A campaign.

The operator monitored the leak rates for the different wells closely prior to re-abandonment, as shown in the graphs of Fig. 4, and some of them show interesting behavior. Well number 16 (W-16) exhibits a near steady-state leak rate at approximately 7 L/h for a period of nearly five months, and well number 4 (W-04) shows similar behavior with a near constant leak rate of 45 L/h for a three-month period. These two leak rates were therefore chosen for the case study, along with a third, postulated worst-case leak scenario of 120 L/h based on the peak leak rate of well number 8 (W-08).

In addition to leak rates, initial bubble sizes of the leaking gas need to be entered into the software. Predicting initial bubble sizes of leaking gas is challenging, as they are dependent on a number of variables. These variables include, but are not limited to, rheology of the fluid(s), mass flux, surfactant contamination such as oiliness in gas bubbles, horizontal water velocity, sizes of the grains and pore channels in the sediment, size and geometry of defect if the fluid escapes through rock or cement, ambient temperature and pressure (Leifer and Culling, 2010; MacDonald et al., 2002). As data from natural seepage studies indicate that this is an important factor for the ultimate fate of the gas release, it was decided to include a sensitivity analysis for a representative range of initial bubble sizes (Wang and Socolofsky, 2015; Lindo-Atichati et al., 2016; Leifer et al., 2004). As Field A is a good analogue to the Tommeliten seep area, the measured bubble size of 4.5 mm from the Tommeliten seeps was chosen as the characteristic bubble size for the fate analysis. To perform the sensitivity analysis, minimum and maximum size of bubbles were set to 1 and 10 mm diameter. This is consistent with the ranges of bubble sizes reported in various studies of natural gas seeps, including the Leifer and Culling (2010) study in COP, where bubble sizes observed were in the range of 500 to 5200 μm radius, and the field observations at the Shane seep in COP made by Leifer and Boles (2005), where bubble sizes observed were in the range of 200 μm to 1 cm radius.

2.3. Case study B

Case study B is a theoretical oil leak at Field B; a Norwegian oil field located in the southern part of the North Sea at approximately 70 m water depth. Since oil production started here in the 1980s, depletion and compaction of the porous and soft chalk reservoir have caused the seabed to subside, which again has led to failure in the overburden and the consequent sinking of a platform. As the clearance between platform and sea shrunk, the operator decided that all 30 platform wells needed to be permanently plugged and abandoned. Degradation of primary cement, deformation and collapse of wells restricting access, and the fact that there are no less than nine distinct permeable zones in the overburden which all need to be isolated by barriers, complicate the campaign (Straume, 2012). The operator at Field B has therefore been positive to use the field as a test spot for new technology and PP&A solutions, including an on-going project aiming to verify the Perforate, Wash and Cement (PWC) method and to include a specific verification process for PWC in the new version of NORSOK D-010, which is being drafted in 2019 (Delabroy et al., 2017; Gundersen, 2017). Trials with placing metal-to-metal seals using metal alloy bismuth and thermite have also recently been conducted on Field B, as the first trials on the NCS (Staff, 2017; Skjold, 2017).

The combination of the pre-existing challenging conditions and the implementation of new, experimental technology may prompt an increased well integrity risk. Due to the ongoing PP&A work on Field B, it was considered interesting to use the field as a subject for leak simulations.

As with Field A, leak rates and initial droplet sizes of the simulated release need to be entered into the software. There are not too many studies conducted on the mass flux from individual oil seeps, as the focus of most research is to gain information on the areal implications of seepage, but Johansen et al. (2017) did a specific video survey of two GoM oil seeps at 1200 m water depth. The two vents emitted oil droplets with an average diameter of 5 mm at rates of 1.11 and 0.31 L/h, respectively. Another study at the Mississippi canyon in the GoM used SAR surveys to estimate thickness and extent of oil slicks dividing the area into a grid of surface blocks representing clusters of seeps. The most active cluster of seeps was estimated to leak 0.14 m^3/d, or 5.83 L/h (Garcia-Pineda et al., 2016). Based on these studies and the initial objective of modeling small hydrocarbon leaks from wells, three leak rates were chosen for modeling: a worst case scenario of 1.0 L/h and two smaller rates of 0.1 L/h and 0.01 L/h.

Four different droplet sizes were chosen for the sensitivity analysis. To calculate droplet size distribution, OSCAR is using the Rosin-Rammler distribution function, which is the most commonly used equation for describing particle size distributions (Gonzalez-Tello et al., 2008). Using the default settings, the characteristic diameter of droplets is set to 3 mm with the size-spread parameter 1.7999. In addition to using the default setting, uniform droplet sizes of 1, 5 and 10 mm were chosen for the sensitivity analysis. This is in line with Garcia-Pineda et al. (2016) defining natural seeping oil and gas to normally be in the range of 1–10 mm in diameter, with Leifer and MacDonald (2003) measuring 1 cm drops of oil expelled in the GoM and the aforementioned GoM video survey of 5 mm droplets emerging from the seafloor.

3. Results and discussions

3.1. Case study A

Released gas bubbles will have a density considerably smaller than the surrounding water, and the resulting buoyancy forces will drive the bubbles upwards with rise velocity v. The following expression for the rise velocity can be derived from Stokes' law:

$$\vartheta = \frac{2(\rho_f - \rho_p)}{9\,\mu} g R^2$$

where ρ_p and ρ_f are the density of the gas particles and the seawater fluid, respectively, g is the gravitational acceleration, R is the radius of a spherical bubble and μ is the dynamic viscosity of the rising fluid. If we assume that the viscosity is constant variable, the rise velocity then becomes a function of bubble size. The seeping gas will also be affected by local currents, and thereby gain a horizontal velocity. Consequently, the seeping gas will reach surface some distance from the release point. When bubbles of different sizes are released under the same conditions, the distance travelled from the wellbore becomes a function of initial bubble size.

To capture all the released gas in the simulations, it is important to have a grid large enough to include the points where gas may either reach surface or dissolve in the water. By trial and error, a grid size of 200 m × 200 m was chosen. To achieve satisfactory temporal resolution, the duration of simulations was set to 24 h for each well. According to the output, the gas rate through surface, or gas mass flux, quickly established a more or less constant rate after t = 0 h and remained in the same interval throughout 24 h. It is therefore believed that 24 h simulations are adequate to capture temporal variations.

Mass balance results for the three leaking wells using the characteristic, initial bubble size of 4.5 mm diameter are presented in Table 1.

The obtained results show that near all gas dissolves in the water

Table 1
Fractions of gas dissolved and released to atmosphere as function of leak rates.

		Winter		Summer	
Well	Leak rate	% of gas dissolved	% of gas to atmosphere	% of gas dissolved	% of gas to atmosphere
W-04	**45 L/h**	99.709%	0.291%	99.924%	0.076%
W-08	**120 L/h**	99.708%	0.292%	99.918%	0.082%
W-16	**7 L/h**	99.711%	0.289%	99.925%	0.075%

while ascending through the water column. The mass balance results do not vary more than 0.003% for the three different wells, even though the factor between the smallest and largest leak rate is more than 17. Based on these results, it is believed that the fraction of gas reaching atmosphere by bubble-mediated transport is independent of flow rate, at least for the rates presented in this case. There are, however, seasonal variations present. In general, more gas reaches the atmosphere in winter than in summer, when degree of vertical mixing is high and no thermocline is present to trap the seeping gas below it. The mass balance is also dependent on the initial bubble sizes, as shown by the results presented in Table 2.

For the expected bubble sizes, simulations show that between 0 and ~4.5% of the leaking gas has the potential of reaching the atmosphere by bubble-mediated transport. The percentage increases with increasing bubble size. When a gas bubble rises through the water column, an exchange of gases will take place. As seawater is highly undersaturated in methane, methane will easily dissolve in the water column, while other gases present in the seawater, such as nitrogen (N_2) and oxygen (O_2) will enter the bubble. Together with partial pressure and initial bubble size, the bubble-water contact time is one of the most important parameters for this gas exchange (McGinnis et al., 2006). The obtained results are in line with this existing theory; the larger bubbles have greater rise velocity, and it follows that the bubble-water contact time decreases while the atmospheric fraction increases. Intuitively, water depth of leaking wells will also be an important factor for the mass balance results. It is likely that for fields with larger water depth than Field A's 70 m, nearly all gas from leaking wells will dissolve in the water. Still, there are some factors that might affect the atmospheric fraction.

During a survey in the GoM, Solomon et al. (2009) found considerable methane fluxes to the atmosphere originating from seeps at 550–600 m water depth. A combination of large flow rate from the seeps and oil coated gas bubbles resulted in very efficient transport to the atmosphere. It is shown that heavy seepage of natural gas can reduce the hydrostatic pressure of the water column, causing an upwelling of flow of both water and gas in a natural gas bubble plume (Clark et al., 2003). Increased rise velocity decreases bubble-water contact time, and increasing levels of dissolved methane in the plume can slow down or completely stop the gas exchange over the bubble surface (Leifer and MacDonald, 2003; Washburn et al., 2005). Gas exchange may also be limited if gas bubbles are covered with an oily coating, a hydrate coating or other surface contamination such as bacteria or microorganisms, as this limits interaction between gas and surrounding seawater (Judd and Hovland, 2007). It is evident that the fate of leaking gas is dependent on numerous parameters, and even though plume dynamics is not addressed further, it is important to clarify that in the case of a substantially increased leak rate, one cannot expect the same, high dissolution rates as presented here.

The results from Field A simulations and the investigations from the Tommeliten seepage area are well suited for comparison, as the water depth, currents and temperature profiles are similar. Schneider von Deimling et al. (2011) estimated that less than 4% of the Tommeliten seeping gas reaches the upper, mixed water layers during the summer months, from where it can escape to the atmosphere. No estimation was made for the winter months, as research cruises in mid-latitude areas tend to take place in summer. The researchers did however mention that the atmospheric fraction might increase when the thermocline breaks down in the colder periods. As a result, the methane flux to the atmosphere may be underestimated. Modeling on different bubble sizes was also performed, with the same trend found of atmospheric transport increasing with increased bubble size. It is interesting that the atmospheric fractions from Field A and Tommeliten seepage area are comparable in size, when the worst-case leak rate from Field A at 120 L/h only makes up ~2.7% of the total emission from the thermogenic, Tommeliten seepage.

In addition to bubble-mediated transport, dissolved natural gas may also reach the atmosphere by diffusion from the mixed layer or by turbulent air-sea gas exchange (Leifer and Patro, 2002). This is not addressed by the software. On a larger time scale, the atmospheric fraction of leaking gas may therefore increase. This was also the conclusion of a team of researchers that investigated exploration wells on the NCS as potential leak paths for shallow, biogenic gas. They estimated that bubble-mediated transport would carry less than 2% of the leaking gas to the atmosphere, but suggested that the actual percentage when including diffusion could reach 42% (Vielstadte et al., 2015, 2017). Clearly there is a huge discrepancy between these numbers, and more effort should be made in developing precise models for predicting ultimate fate of leaking gas, especially since being able to accurately evaluate the consequences of leaking wells rely on it.

Reviewing potential harmful effects of gas leaks from abandoned wells is made quite easy by the large amount of literature available on natural gas seepage. Research is often focused on methane, the lightest and most abundant component of natural gas. The interest is sparked by the fact that methane is a potent greenhouse gas, with a global warming potential 25 times that of carbon dioxide (CO_2) (Yvon-Durocher et al., 2014; Reeburgh, 2007). When Vielstadte et al. (2017) attempted to quantify the potential leakage of biogenic gas from wells on the NCS, their worst case scenario including diffusion concluded that 7000 t of methane could be released to the atmosphere annually. This number could be put into perspective by Reeburgh (2007), who estimated the global, annual methane flux to the atmosphere to be 545 Tg per year, or 535 million t per year.

The largest fraction of the released gas ends up dissolved in the seawater. Again, there is a lot of literature available from studies of natural seepage. As previously mentioned, dissolved gas will be subject to mostly aerobic biodegradation in the water column by bacteria utilizing O_2 to create CO_2 as a typical end product (Reeburgh, 2007; Judd

Table 2
Fractions of gas released to atmosphere and gas dissolved as function of initial bubble size for W-16.

	Winter		Summer	
Initial bubble size	% of gas dissolved	% of gas to atmosphere	% of gas dissolved	% of gas to atmosphere
1 mm	100.00%	0.000%	100.00%	0.000%
4.5 mm	97.108%	0.289%	99.925%	0.075%
10 mm	95.510%	4.490%	96.029%	3.971%

and Hovland, 2007). On a large scale, this depletion of oxygen and enrichment of CO_2 can contribute to the processes of ocean acidification and oxygen depletion (Biastoch et al., 2011). Lowering the pH of the ocean and disturbing chemical balances can be very problematic, as it may directly affect marine organisms part of sensitive ecosystems. Ultimately, humans and animals alike are all dependent on the massive food source and source of livelihood the oceans represents (Doney et al., 2009). However, the main driver for these effects is anthropogenic sources of atmospheric CO_2 by the burning of fossil fuels, as approximately one third is absorbed by the oceans by diffusion. It is unlikely that the leaking wells in Field A would contribute in a size order with much impact.

It is known that in areas of high seepage, benthic communities including methane-oxidizing microorganisms thrive, and bacterial mats are commonly found on the seabed. This can attract fish and other macro-fauna, providing them with food and enriching the food chain (Hovland, 2008; Hovland et al., 2012). In the Gullfaks seepage area, one of Norway's most heavily fished areas, hermit crabs have been observed fighting over pieces of bacterial mat (Hovland, 2007). The environmental effects of dissolved gas in the ocean due to leaking wells is clearly a multi-faceted issue, and something that would be interesting to study further.

3.2. Case study B

When investigating the fate of oil from a leaking well, the first question that arises is where the oil will go and how it will be divided into different fractions in the environment. In the software, the mass balance is represented by a graph of percentages denoting weight percent. To analyze the mass balance during a constant leak from a well, simulations for the three different leak rates were performed for both winter and summer scenarios with all the four different droplet size distributions. In total, this makes 24 simulations and provides a foundation for evaluating seasonal variations and the importance of initial droplet size and leak rate. The simulations were set up with constant leak rate for 90 days with a simulation grid of 200 km × 200 km.

The mass balance results are cumulative numbers, with the percentages of the different fractions including all released oil from t = 0 until time t. In the beginning of the simulation, the dominating fraction will therefore be oil in the water column, whereas the final fractions at day 90 will be dominated by the fractions describing the ultimate fate of the oil, such as oil evaporated to the atmosphere, biodegraded oil and oil deposited in the sediments. In a way, these three fractions describe the "end stations" of the release. The results are shown in Fig. 5.

As oil is generally not soluble in water, it will move with the surrounding water masses and persist in the environment for quite some time, possibly traveling large distances. This is evident by the fact that ~4.5% and ~13% escapes the grid in summer and winter, respectively, noted by the fraction named *Outside* in Fig. 5. In this way, oil leaking from a well in one sector of the North Sea may travel into another country's sector, affecting the environment of other countries as well.

Fig. 5 shows the results from the simulations with leak rate 1.0 L/h. As with case study A, it was found that the mass balance results are independent on the leak rates from the well. This is perhaps not unintuitive when we consider that leak rates between 0.01 and 1.0 L/h are effectively spread out over an area of several hundred kilometers. Differences in results based on different leak rates will therefore not be addressed further.

More obvious are seasonal variations and which fractions are dependent on initial droplet size. To accurately analyze this, new simulations were set up to gain information on the ultimate fractions of the oil leaks. For the new simulations, the releases were set to last for five days with the simulations running for 90 days. The grid was expanded to 400 km × 400 km in order to capture all the oil. The simulations were only performed using one leak rate of 0.1 L/h, as previous results showed no variation in results with leak rate. The results are presented in Fig. 6.

From the graph, it is apparent that the atmospheric and biodegraded fractions are both dependent on the initial droplet size, and are inversely dependent on each other. This is consistent with literature on natural seepages and other releases. Larger droplets rise quicker and thus transports the oil more efficiently to surface, from where it may evaporate. Smaller droplets experience a greater droplet-water contact time and have a larger surface area compared to the volume, favoring dissolution and biodegradation. Consequently, the atmospheric fraction increases with increasing droplet size while the biodegraded fraction simultaneously decreases. In fact, this is the reason why chemical dispersants are commonly used in cleanups of accidental oil spills in areas where surface oil pose a risk to the environment (Li et al., 2016). A study by Brakstad et al. (2015), who investigated the biodegradation rates of

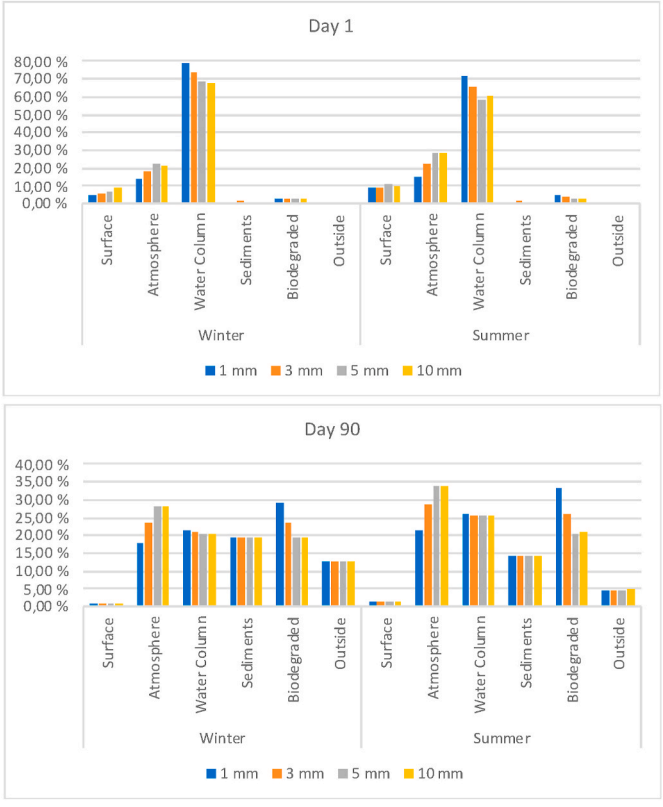

Fig. 5. Mass balance results for the leak rate of 1.0 L/h as function of season and initial droplet size.

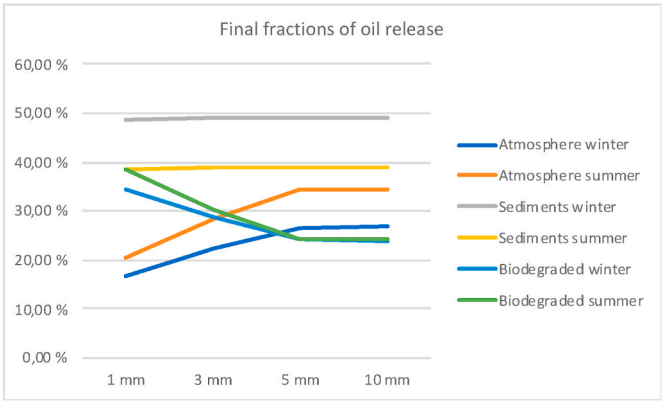

Fig. 6. Final mass balance according to season and initial droplet size.

Macondo oil in Norwegian seawater at low temperature, showed improved biodegradation rates after dispersant treatments of oil, in line with our results. It is also interesting to note that the results for 5 and 10 mm droplets are approximately the same, leaving us to believe that modeling even greater droplet sizes is not necessary.

Seasonal variations are also visible in Fig. 6. Both atmospheric and biodegraded fractions are larger in summer than in winter. Higher atmospheric temperature increases evaporation, and more sunlight and warmer water speeds up biodegradation rates (Fingas, 2011). As a result, the sediment fraction decreases during summer and increases during winter. It is apparent that the sediment fraction is a function of chemical composition of the oil and the ambient temperature. As previously stated, the sediment fraction consists of the heaviest oil compounds and those most resistant to biodegradation. The seasonal variations indicate that some of the oil compounds present in Field B oil are only willing to enter gaseous phase when subject to summer temperatures.

After having established the ultimate fate of the oil released, it is interesting to see how the mass balance results are also functions of time. From Fig. 7, we can see that after a five day leak from a well, oil will be present submerged in the water either as droplets or dissolved oil for approximately 25 days in winter and 60+ days in summer before reaching an end station. Oscillating values for surface oil can also be observed during the first few days, as a sign of varying weather and wave activity.

If we look closer at the sediment fractions, a slight downwards slope is noticeable. This represents the biodegradation rates within the sediments. To investigate this further, the winter simulation of a five-day release was extended for a full year. During that time, the sediment fraction dropped from approximately 50%–22% by the end of the year. This indicates that oil in the sediments can be present for a couple of years after a release, even after a short release with low leak rate.

After analyzing how the oil fractionates in the environment, the next important part of the oil fate analysis is to evaluate the concentration

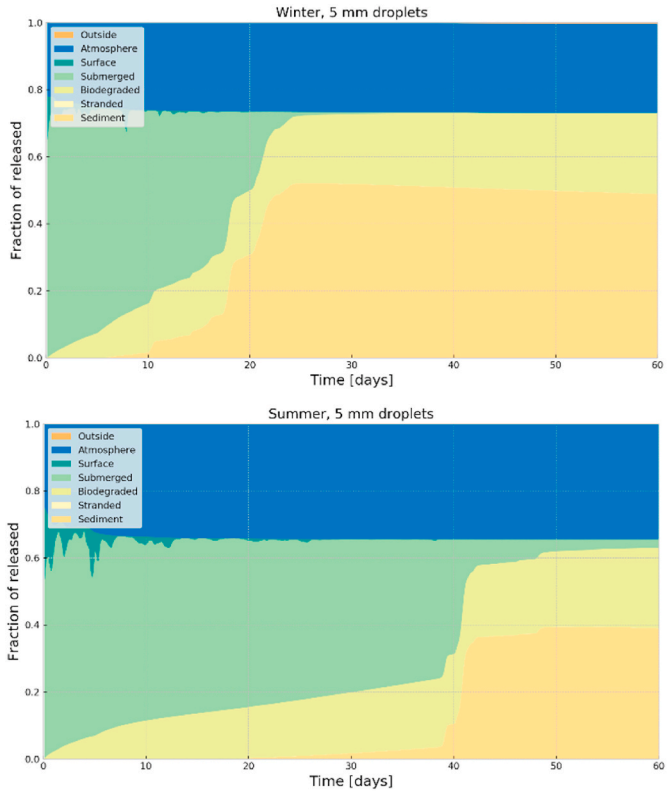

Fig. 7. Mass balance results as function of time following a five-day oil release.

Table 3
Mean and maximum concentrations (in water and sediment) following the release scenarios.

Release rate	Droplet size	Winter		Summer	
		Mean conc.	Max. conc.	Mean conc.	Max conc.
0.01 L/h	**1 mm**	0.017 ppb	1.863 ppb*	0.010 ppb	2.259 ppb
	3 mm	0.007 ppb	0.950 ppb	0.006 ppb	0.779 ppb
	5 mm	0.005 ppb	0.664 ppb	0.004 ppb	0.429 ppb
	10 mm	0.004 ppb	0.377 ppb	0.003 ppb	0.261 ppb
0.1 L/h	**1 mm**	0.147 ppb	20.07 ppb	0.099 ppb	17.72 ppb
	3 mm	0.057 ppb	10.64 ppb	0.048 ppb	7.512 ppb
	5 mm	0.051 ppb	6.726 ppb	0.039 ppb	4.457 ppb
	10 mm	0.037 ppb	3.346 ppb	0.024 ppb	2.624 ppb
1.0 L/h	**1 mm**	1.418 ppb	198.09 ppb*	0.993 ppb	255.1 ppb
	3 mm	0.521 ppb	101.6 ppb	0.427 ppb	74.08 ppb
	5 mm	0.482 ppb	53.72 ppb	0.363 ppb	44.15 ppb
	10 mm	0.332 ppb	45.97 ppb	0.225 ppb	23.01 ppb

data. Concentrations of oil in water and sediment are the most important factors controlling the toxicity of a release, besides the chemical composition of the oil. As the highest concentrations are expected in close proximity to the wellbore, a grid of 500 m × 500 m was chosen with individual cells being 5 m × 5 m in the horizontal plane and 8 m in the vertical direction. Durations and the simulations of the release were both set to five days, and simulations were run for all leak rates in winter and summer with all droplet size distributions, 24 simulations in total. Results are presented in Table 3, where mean concentrations are average values of all mean concentrations for every computational time step during the simulation. Maximum concentration values are denoting the absolute maximum concentration achieved in a single grid cell during any time t of the simulation. In general, concentration data includes all of the submerged oil, including dissolved oil, oil suspended as droplets and oil in emulsion with water.

From the obtained results, it is indicated that increasing the leak rate by a factor of 10 also causes the mean and maximum concentrations to increase by a similar factor. Not surprisingly, the concentrations also tend to increase with decreasing initial droplet size and are higher in winter than in summer. The maximum value of mean concentration is therefore obtained at the highest leak rate of 1.0 L/h combined with the smallest droplet size of 1 mm during winter.

4. Conclusions

4.1. Gas leakage

In the case of gas leaks from permanently abandoned wells on Field A, simulations showed that the fraction of gas able to reach the atmosphere by bubble-mediated transport is very low, and approximately 95–99% of the released gas will dissolve in the sea. Results are consistent with data from the Tommeliten natural seepage area. However, the ultimate atmospheric fraction might be higher on a long-term scale, as increased methane concentrations in the sea may cause methane to reach the atmosphere by diffusion from seawater. These effects are not addressed by the software and should be investigated further to be able to evaluate the environmental impact, as natural gas reaching the atmosphere may contribute to local air pollution and global warming.

Natural gas being biodegraded by marine organisms, although serving as a nutrient for marine life and possibly enriching the food chain, may contribute to the effects of oxygen depletion and ocean acidification, as O_2 is utilized and CO_2 produced. Calculations show that the leak rates from Field A are small compared to the natural seepage at Tommeliten.

Sensitivity analyses showed that the fate of the leaking gas is dependent on the initial bubble sizes of the release and seasonal variations. The fraction of gas reaching the atmosphere increases with increasing bubble size and is higher in winter when there is no thermocline present. Analyses also show that for the leak rates in question, the fate of the gas is independent on the leak rate.

4.2. Oil leakage

In the case of oil leaks from permanently abandoned wells, the oil undergoes a weathering process and become fractionated in the environment. Ultimately, the oil will either evaporate to the atmosphere, be biodegraded by marine organisms or be deposited on the seafloor sediments or hit the shore. During constant leakage from a well, some oil may also be present on surface in the form of surface slicks or be suspended in the water as either emulsion, droplets or dissolved oil. In addition to relying greatly on the chemical composition of the oil, sensitivity analyses show that the fate of the leaking oil is dependent on the initial droplet sizes of the release and seasonal variations.

The ranges of the typical mass balance results for an oil leak at Field B show that 17–34% of the oil evaporates, 24–38% is biodegraded and 39–49% is deposited on the seafloor sediments. Due to its persistent nature, oil may travel over large distances with the prevailing currents, and thereby affect areas several hundred kilometers away from the release point. Biodegradation rates in the sediments are slow, and oil may persist in the environment for years after release. When biodegraded, oil compounds may accumulate in the food chain, but as there are no available data from oil seepage on the NCS, possible long-term effects of leaking wells are not yet well understood.

The toxicity of oil in water or in the sediments is dependent on the concentrations of the oil, the chemical composition and the relative concentration of the most toxic compounds in either water or sediments. Further research on this matter is needed if threshold values for leaking wells on the NCS are to be defined.

Credit author statement

Mari R. Tveit: Methodology, Software, Data curation, Writing. Mahmoud Khalifeh: Conceptulization, Methodology, Review and Editing, Supervison, Project adminstration. Tor Nordam: Software, Reviewing and Editing. Arild Saasen: Supervision, Methodology, Reviewing & Editing.

Declaration of competing interest

The authors declare that they have no known competing financial interests or personal relationships that could have appeared to influence the work reported in this paper.

Acknowledgments

The authors would like to thank ConocoPhillips, Equinor, AkerBP, and Norwegian P&A forum (PAF) for giving fruitful input. The authors also would like to thank ASME for granting the permission to publish the paper at the journal of Petroleum Science and Engineering.

Appendix A. Supplementary data

Supplementary data to this article can be found online at https://doi.org/10.1016/j.petrol.2020.108004.

References

Audunson, T., 1980. The fate and weathering of surface oil from the bravo blowout. Mar. Environ. Res. 3 (1), 35–61. https://doi.org/10.1016/0141-1136(80)90034-3.

Bagi, Andrea, Pampanin, Daniela M., Gunnar Brakstad, Odd, Kommedal, Roald, August 2013. Estimation of hydrocarbon biodegradation rates in marine environments: A critical review of the Q_{10} approach. Mar. Environ. Res. 89, 83–90.

Barclay, I., Pellenberg, J., Tettero, F., et al., 2001. The beginning of the end: a review of abandonment and decommissioning practices. Oilfield Rev. 13 (4), 28–41.

Bernard, B.B., Brooks, J.M., Sackett, W.M., 1978. Light hydrocarbons in recent Texas continental shelf and slope sediments. J. Geophys. Res.: Oceans 83 (C8), 4053–4061. https://doi.org/10.1029/JC083iC08p04053.

Biastoch, A., Treude, T., Rüpke, L.H., et al., 2011. Rising Arctic Ocean temperatures cause gas hydrate destabilization and ocean acidification. Geophys. Res. Lett. 38 (8), 1–5. https://doi.org/10.1029/2011GL047222.

Brakstad, O.G., Nordtug, T., Throne-Holst, M., 2015. Biodegradation of dispersed Macondo oil in seawater at low temperature and different oil droplet sizes. Mar. Pollut. Bull. 93 (1), 144–152. https://doi.org/10.1016/j.marpolbul.2015.02.006.

Brooks, J.M., Bernard, B.B., Sackett, W.M., et al., 1979. Natural Gas Seepage on the South Texas Shelf. In: Presented at the Offshore Technology Conference. https://doi.org/10.4043/3411-MS. Houston, Texas, April 30 - May 3. OTC-3411-MS.

Bünz, S., Polyanov, S., Vadakkepuliyambatta, S., et al., 2012. Active gas venting through hydrate-bearing sediments on the Vestnesa Ridge, offshore W-Svalbard. Mar. Geol. 332–334, 189–197. https://doi.org/10.1016/j.margeo.2012.09.012.

Campbell, K., Smith, R., 2013. Permanent well Abandonment. Way 9 (3), 25–27. https://doi.org/10.2118/0313-025-TWA. SPE-0313-025-TWA.

Chand, S., Rise, L., Dolan, M., et al., 2008. Active venting system offshore northern Norway. Eos, Transactions American Geophysical Union 89 (29), 261–262. https://doi.org/10.1029/2008EO290001.

Clark, J.F., Leifer, I., Washburn, L., et al., 2003. Compositional changes in natural gas bubble plumes: observations from the Coal Oil Point marine hydrocarbon seep field. Geo Mar. Lett. 23 (3), 187–193. https://doi.org/10.1007/s00367-003-0137-y.

Delabroy, L., Rodrigues, D., Norum, E., et al., 2017. Perforate, Wash and Cement PWC Verification Process and an Industry Standard for Barrier Acceptance Criteria. Presented at the SPE Bergen One Day Seminar, Bergen, Norway, 5 April. https://doi.org/10.2118/185938-MS. SPE-185938-MS.

Doney, S.C., Fabry, V.J., Feely, R.A., et al., 2009. ocean acidification: the other CO2 problem. Annual Review of Marine Science 1 (1), 169–192. https://doi.org/10.1146/annurev.marine.010908.163834.

Etiope, G., 2015. Natural Gas Seepage, 1. Springer International Publishing (Reprint), Switzerland.

Evans, G.W., Carter, L.G., 1962. Bounding studies of cementing compositions to pipe and formations. In: Presented at the Drilling and Production Practice, New York, New York, 1 January. API-62-072.

Faksness, L.-G., Brandvik, P.J., Daling, P.S., et al., 2016. The value of offshore field experiments in oil spill technology development for Norwegian waters. Mar. Pollut. Bull. 111 (1), 402–410. https://doi.org/10.1016/j.marpolbul.2016.07.035.

Farwell, C., Reddy, C.M., Peacock, E., et al., 2009. Weathering and the fallout plume of heavy oil from strong petroleum seeps near coal oil point, CA. Environ. Sci. Technol. 43 (10), 3542–3548. https://doi.org/10.1021/es802586g.

Fingas, M., 2011. Oil Spill Science and Technology : Prevention, Response, and Cleanup. Gulf Professional Publishing (Reprint), Burlington, Mass.

Fronks, R.C., 2002. International regulations - meeting the challenge. In: Presented at the SPE International Conference on Health, Safety and Environment in Oil and Gas Exploration and Production. Kuala Lumpur, Malaysia, pp. 20–22. https://doi.org/10.2118/73879-MS. March. SPE-73879-MS.

Garcia-Pineda, O., MacDonald, I., Silva, M., et al., 2016. Transience and persistence of natural hydrocarbon seepage in Mississippi Canyon, Gulf of Mexico. Deep Sea Res. Part II Top. Stud. Oceanogr. 129, 119–129. https://doi.org/10.1016/j.dsr2.2015.05.011.

Gasda, S.E., Bachu, S., Celia, M.A., 2004. Spatial characterization of the location of potentially leaky wells penetrating a deep saline aquifer in a mature sedimentary basin. Environ. Geol. 46 (6), 707–720. https://doi.org/10.1007/s00254-004-1073-5.

Geoconsulting, C.G.G., 2015. Figure: Combined Coverage of GLOGOS, FFD and FRogi Seeps, Adding Verification Data to the Global Offshore Seepage Database. https://www.cgg.com/en/Media-and-Events/Media-Releases/2015/12/CGG-GeoConsulting-Introduces-Seep-Explorer-and-GLOGOS.

Geyer, R.A., Sweet Jr., W.E., 1972. Natural hydrocarbon seepage in the Gulf of Mexico. In: Presented at the SPE Symposium on Environmental Conservation, Lafayette, Louisiana, 13-14 November. SPE-4199-MS. https://doi.org/10.2118/4199-MS.

González-Tello, P., Camacho, F., Vicaria, J.M., et al., 2008. A modified Nukiyama–Tanasawa distribution function and a Rosin–Rammler model for the particle-size-distribution analysis. Powder Technol. 186 (3), 278–281. https://doi.org/10.1016/j.powtec.2007.12.011.

Gundersen, J., 2017. Regulatory «Updates». Presented at the Plug and Abandonment Forum (PAF) Seminar, Sola, Norway, 18 October. https://norskoljeoggass.no/globalassets/dokumenter/drift/presentasjonerarrangementer/plug–abandonment-seminar-2017/04-regulatory-updates—johnny-gundersen-psa-20171022192327.pdf.

Hornafius, J.S., Quigley, D., Luyendyk, B.P., 1999. The world's most spectacular marine hydrocarbon seeps (Coal Oil Point, Santa Barbara Channel, California): quantification of emissions. J. Geophys. Res.: Oceans 104 (C9), 20703–20711. https://doi.org/10.1029/1999JC900148.

Hovland, M., 2007. Discovery of prolific natural methane seeps at Gullfaks, northern North Sea. Geo Mar. Lett. 27 (2), 197–201. https://doi.org/10.1007/s00367-007-0070-6.

Hovland, M., 2008. Deep-water Coral Reefs : Unique Biodiversity Hot-Spots. Springer Netherlands, Chichester, UK.
Hovland, M., Sommerville, J.H., 1985. Characteristics of two natural gas seepages in the North Sea. Mar. Petrol. Geol. 2 (4), 319–326. https://doi.org/10.1016/0264-8172(85)90027-3.
Hovland, M., Jensen, S., Fichler, C., 2012. Methane and minor oil macro-seep systems — their complexity and environmental significance. Mar. Geol. 332–334, 163–173. https://doi.org/10.1016/j.margeo.2012.02.014.
IEA GHG, 2009. IEA Greenhouse Gas R&D Programme, Long Term Integrity of CO2 Storage – Well Abandonment. Report No. 2009/08. Ch. 5 - Well abandonment regulations (July 2009).
Johansen, C., Todd, A.C., MacDonald, I.R., 2017. Time series video analysis of bubble release processes at natural hydrocarbon seeps in the Northern Gulf of Mexico. Mar. Petrol. Geol. 82, 21–34. https://doi.org/10.1016/j.marpetgeo.2017.01.014.
Judd, A., 2004. Natural seabed gas seeps as sources of atmospheric methane. Environ. Geol. 46 (8), 988–996. https://doi.org/10.1007/s00254-004-1083-3.
Judd, A., Hovland, M., 2007. Seabed Fluid Flow: the Impact on Geology, Biology, and the Marine Environment. Cambridge University Press (Reprint), Cambridge.
Khalifeh, M., Gardner, D., Haddad, M.Y., 2017. Technology Trends in Cement Job Evaluation Using Logging Tools. Presented at the Abu Dhabi International Petroleum Exhibition & Conference, Abu Dhabi, UAE, 13-16 November. https://doi.org/10.2118/188274-MS. SPE-188274-MS.
Khalifeh, M., Hodne, H., Saasen, A., et al., 2018. Bond strength between different casing materials and cement. Presented at the SPE Norway One Day Seminar, Bergen, Norway, 18 April. https://doi.org/10.2118/191322-MS. SPE-191322-MS.
Kvenvolden, K.A., Cooper, C.K., 2003. Natural seepage of crude oil into the marine environment. Geo Mar. Lett. 23 (3–4), 140–146. https://doi.org/10.1007/s00367-003-0135-0.
Leifer, I., Boles, J., 2005. Measurement of marine hydrocarbon seep flow through fractured rock and unconsolidated sediment. Mar. Petrol. Geol. 22 (4), 551–568. https://doi.org/10.1016/j.marpetgeo.2004.10.026.
Leifer, I., Culling, D., 2010. Formation of seep bubble plumes in the Coal Oil Point seep field. Geo Mar. Lett. 30 (3), 339–353. https://doi.org/10.1007/s00367-010-0187-x.
Leifer, I., MacDonald, I., 2003. Dynamics of the gas flux from shallow gas hydrate deposits: interaction between oily hydrate bubbles and the oceanic environment. Earth Planet Sci. Lett. 210 (3), 411–424. https://doi.org/10.1016/S0012-821X(03)00173-0.
Leifer, I., Patro, R.K., 2002. The bubble mechanism for methane transport from the shallow sea bed to the surface: a review and sensitivity study. Continent. Shelf Res. 22 (16), 2409–2428. https://doi.org/10.1016/S0278-4343(02)00065-1.
Leifer, I., Boles, J.R., Luyendyk, B.P., et al., 2004. Transient discharges from marine hydrocarbon seeps: spatial and temporal variability. Environ. Geol. 46 (8), 1038–1052. https://doi.org/10.1007/s00254-004-1091-3.
Lende, G., 2012. Advances in Cementing Technology for Permanent P&A, Halliburton. Presented at the Plug and Abandonment Forum (PAF) Seminar, Sola, Norway, 14. June. https://www.norskoljeoggass.no/drift/presentasjonerarrangementer/plug–abandonment-seminar-2012/.
Li, P., Cai, Q., Lin, W., et al., 2016. Offshore oil spill response practices and emerging challenges. Mar. Pollut. Bull. 110 (1), 6–27. https://doi.org/10.1016/j.marpolbul.2016.06.020.
Lindo-Atichati, D., Paris, C.B., Le Hénaff, M., et al., 2016. Simulating the effects of droplet size, high-pressure biodegradation, and variable flow rate on the subsea evolution of deep plumes from the Macondo blowout. Deep Sea Res. Part II Top. Stud. Oceanogr. 129, 301–310. https://doi.org/10.1016/j.dsr2.2014.01.011.
Link, W.K., 1952. Significance of oil and gas seeps in world oil exploration. AAPG (Am. Assoc. Pet. Geol.) Bull. 36 (8), 1505–1540.
Liversidge, D., Taoutaou, S., Agarwal, S., 2006. Permanent plug and abandonment solution for the North sea. In: Presented at the SPE Asia Pacific Oil & Gas Conference and Exhibition, Adelaide, Australia, pp. 11–13. https://doi.org/10.2118/100771-MS. September. SPE-100771-MS.
Logan, G.A., Jones, A.T., Kennard, J.M., et al., 2010. Australian offshore natural hydrocarbon seepage studies, a review and re-evaluation. Mar. Petrol. Geol. 27 (1), 26–45. https://doi.org/10.1016/j.marpetgeo.2009.07.002.
MacDonald, I.R., Leifer, I., Sassen, R., et al., 2002. Transfer of hydrocarbons from natural seeps to the water column and atmosphere. Geofluids 2 (2), 95–107. https://doi.org/10.1046/j.1468-8123.2002.00023.x.
McGinnis, D.F., Greinert, J., Artemov, Y., et al., 2006. Fate of rising methane bubbles in stratified waters: how much methane reaches the atmosphere? J. Geophys. Res.: Oceans 111 (9), 1–15. https://doi.org/10.1029/2005JC003183.
Mikolaj, P.G., Allen, A.A., Schlueter, R.S., 1972. Investigation of the Nature, Extent and Fate of Natural Oil Seepage off Southern California. In: Presented at the Offshore Technology Conference. https://doi.org/10.4043/1549-MS. Houston, Texas, May 1-3. OTC-1549-MS.
Mohammedyasin, S.M., Lippard, S.J., Omosanya, K.O., et al., 2016. Deep-seated faults and hydrocarbon leakage in the Snøhvit gas field, hammerfest basin, Southwestern Barents sea. Mar. Petrol. Geol. 77, 160–178. https://doi.org/10.1016/j.marpetgeo.2016.06.011.
National Research Council (U.S, 2003. Oil in the Sea III: Inputs, Fates, and Effects. National Academy Press (Reprint), Washington, D.C.
Nelson, E.B., Guillot, D., 2006. Well Cementing, second ed. Schlumberger (Reprint), Sugar Land, Texas, USA.
Nissanka, I.D., Yapa, P.D., 2017. Oil slicks on water surface: breakup, coalescence, and droplet formation under breaking waves. Mar. Pollut. Bull. 114 (1), 480–493. https://doi.org/10.1016/j.marpolbul.2016.10.006.
Nordam, Tor, Lofthus, Synnøve, Gunnar Brakstad, Odd, September 2020. Modelling biodegradation of crude oil components at low temperatures. Chemosphere 254, 126836.
NORSOK Standard, D.-010, 2013. Well integrity in drilling and well operations. Rev. 4. 2013. Lysaker, Norway: Standards Norway.
Oil, Gas, U.K., 2012a. Guidelines for the Suspension and Abandonment of Wells. Issue 4. 2012. The UK Offshore Oil and Gas Industry Association Limited, Great Britain.
Oil, Gas, U.K., 2012b. Guidelines on Qualification of Materials for the Suspension and Abandonment of Wells. Issue 1. 2012. The UK Offshore Oil and Gas Industry Association Limited, Great Britain.
Olsen, J.E., Dunnebier, D., Davies, E., et al., 2017. Mass transfer between bubbles and seawater. Chem. Eng. Sci. 161, 308–315. https://doi.org/10.1016/j.ces.2016.12.047.
Pohlmann, T., 1996. Calculating the annual cycle of the vertical eddy viscosity in the North Sea with a three-dimensional baroclinic shelf sea circulation model. Continent. Shelf Res. 16 (2), 147–161. https://doi.org/10.1016/0278-4343(94)E0037-M.
Reeburgh, W.S., 2007. Oceanic methane biogeochemistry. Chem. Rev. 107 (2), 486–513. https://doi.org/10.1021/cr050362v.
Salehi, S., Khattak, M.J., Ali, N., et al., 2016. Development of geopolymer-based cement slurries with enhanced thickening time, compressive and shear bond strength and durability. In: Presented at the IADC/SPE Drilling Conference and Exhibition, Fort Worth, Texas, USA, pp. 1–3. https://doi.org/10.2118/178793-MS. March. SPE-178793-MS.
Schneider von Deimling, J., Rehder, G., Greinert, J., et al., 2011. Quantification of seep-related methane gas emissions at Tommeliten, North Sea. Continent. Shelf Res. 31 (7), 867–878. https://doi.org/10.1016/j.csr.2011.02.012.
Schoell, M., 1980. The hydrogen and carbon isotopic composition of methane from natural gases of various origins. Geochem. Cosmochim. Acta 44 (5), 649–661. https://doi.org/10.1016/0016-7037(80)90155-6.
SINTEF, 2017. SINTEF MEMW (Marine Environmental Modeling Workbench) User's Manual. Version 9.0.0 (8 June 2017).
Skjold, M., 2017. Update Alternative P&A Barrier, Interwell. Presented at the Plug and Abandonment Forum (PAF) Seminar, Sola, Norway, 18 October. https://www.norskoljeoggass.no/drift/presentasjonerarrangementer/plug–abandonment-seminar-2017/.
Slagstad, Dag, McClimans, Thomas A., October 2005. Modeling the ecosystem dynamics of the Barents sea including the marginal ice zone: I. Physical and chemical oceanography. J. Mar. Syst. 58 (1–2), 1–18.
Smith, I., Olstad, D., Segura, R., 2011. Heightened regulations create demand for well abandonment services. Offshore 71 (10), 70–73.
Solomon, E.A., Kastner, M., MacDonald, I.R., et al., 2009. Considerable methane fluxes to the atmosphere from hydrocarbon seeps in the Gulf of Mexico. Nat. Geosci. 2, 561. https://doi.org/10.1038/ngeo574.
SOS California, 2018. Natural oil seepage facts. Stop oil seeps California. http://www.soscalifornia.org/natural-oil-seepage-facts/. (Accessed 25 May 2018).
Staff, O.E., 2017. BiSN Completes Valhall P&A. Offshore Engineer, 13 April 2018. http://www.oedigital.com/subsea/item/16174-bisn-completes-valhall-p-a.
Stolper, D.A., Lawson, M., Formolo, M.J., et al., 2018. The utility of methane clumped isotopes to constrain the origins of methane in natural gas accumulations. Geological Society, London, Special Publications 468 (1), 23. https://doi.org/10.1144/SP468.3.
Straume, M., 2012. Valhall P&A challenges. Presented at the plug and abandonment forum (PAF) seminar, sola, Norway, 14 June. https://www.norskoljeoggass.no/drift/presentasjonerarrangementer/plug–abandonment-seminar-2012/.
Thiercelin, M.J., Dargaud, B., Baret, J.F., et al., 1998. Cement Design Based on Cement Mechanical Response. https://doi.org/10.2118/52890-PA.
Tissot, B.P., Welte, D.H., 1984. Petroleum Formation and Occurrence, 2nd rev. and enlarged ed. Springer (Reprint), Berlin.
Vielstädte, L., Karstens, J., Haeckel, M., et al., 2015. Quantification of methane emissions at abandoned gas wells in the Central North Sea. Mar. Petrol. Geol. 68 (Part B), 848–860. https://doi.org/10.1016/j.marpetgeo.2015.07.030.
Vielstädte, L., Haeckel, M., Karstens, J., et al., 2017. Shallow gas migration along hydrocarbon wells–an unconsidered, anthropogenic source of biogenic methane in the North sea. Environ. Sci. Technol. 51 (17), 10262–10268. https://doi.org/10.1021/acs.est.7b02732.
Vignes, B., 2011. Qualification of well barrier elements - long-term integrity test, test medium and temperatures. In: Presented at the SPE European Health, Safety and Environmental Conference in Oil and Gas Exploration and Production, Vienna, Austria, pp. 22–24. https://doi.org/10.2118/138465-MS. February. SPE-138465-MS.
Wang, B., Socolofsky, S.A., 2015. A deep-sea, high-speed, stereoscopic imaging system for in situ measurement of natural seep bubble and droplet characteristics. Deep Sea Res. Oceanogr. Res. Pap. 104, 134–148. https://doi.org/10.1016/j.dsr.2015.08.001.
Washburn, L., Clark, J.F., Kyriakidis, P., 2005. The spatial scales, distribution, and intensity of natural marine hydrocarbon seeps near Coal Oil Point, California. Mar. Petrol. Geol. 22 (4), 569–578. https://doi.org/10.1016/j.marpetgeo.2004.08.006.
WHOI, 2014. Image : natural oil seeps, illustration by jack cook. http://www.whoi.edu/oilinocean/page.do?pid=51880&tid=441&cid=139413&ct=61&article=97109.
Yvon-Durocher, G., Allen, A.P., Bastviken, D., et al., 2014. Methane fluxes show consistent temperature dependence across microbial to ecosystem scales. Nature 507, 488–491. https://doi.org/10.1038/nature13164.